

Observation of improved and degraded confinement with driven flow on the LAPD

D.A. Schaffner, T.A. Carter, D.S. Guice, J. Maggs, S. Vincena, and B. Friedman
Department of Physics and Astronomy, University of California, Los Angeles.

G.D. Rossi
Department of Physics, University of Texas, Austin
(Dated: April 15, 2012)

Continuous control over the azimuthal flow and flow shear in the edge region of the Large Plasma Device (LAPD) has been achieved using a biasable limiter allowing a detailed study of the effect of flow shear on turbulence and transport in LAPD, extending previous work [1]. LAPD rotates spontaneously in the ion diamagnetic direction (IDD); positive limiter bias allows this spontaneous flow to be reduced, minimized (producing a near-zero flow and flow shear state), and reversed to strong flow in the electron diamagnetic direction (EDD). Confinement or decreases in radial cross-field transport—characterized by turbulent particle flux and density gradient scale length—are shown to vary continuously with shearing rate with confinement degradation observed in the minimum shearing state and confinement improvement in higher shearing states for both IDD and EDD flow directions. Confinement improvement is shown to begin at shearing rates less than the no-shear turbulent autocorrelation rate. This suppression in cross-field transport is dominated by decreases in low-frequency ($\lesssim 10\text{kHz}$) density fluctuations and reduction of radial decorrelation length of turbulent structures. An increase in density fluctuations for the highest shearing states is observed with the emergence of a coherent mode with frequencies $\gtrsim 10\text{kHz}$; however, overall flux is unchanged as isat/E-field crossphase nulls out radial transport. The variations of density fluctuation and radial correlation length are fit to power-law functions for comparison to simple shearing effects models.

The effect of flow and flow shear on plasma turbulence has long been studied as a mechanism for turbulence reduction and increased particle confinement in both tokamaks and linear machines. The most dramatic observed effect of cross-field flow is the creation of a higher confinement state, called an H-mode, which has been first observed on ASDEX[2] and later on other tokamaks such as the Continuous Current Tokamak (CCT)[3, 4] and DII-D[5, 6]. While some plasma machines rely on a spontaneous flow for study[7], other machines including TEXTOR[8] and LAPD[1, 9] have developed external biasing mechanisms to produce radial electric fields which can drive controllable azimuthal flow by $E \times B$ drift[10].

Theoretical investigation into the nature of effect of sheared flow has focused mainly on its influence on turbulent fluctuations [11] and on the crossphase between electric field and any advected quantity, such as density in the case of particle flux [12, 13]. Fluctuation reduction by shear is thought to come by the reduction in radial correlation length—shearing of turbulent eddies—while the effect of crossphase involves the turbulent particle flux dependence on the phasing of outward or inward $E \times B$ flows with density fluctuations. The simplest mode non-specific models for the effect of shearing on turbulent fluctuations predict a power law decrease[11], while crossphase can have an even stronger scaling[13].

Some biasing experiments have been previously conducted on LAPD. In one, an inward pointing electric field produced by chamber biasing demonstrated that increased flow shear resulted in turbulent modification and increased particle confinement[1]. However, penetration of the electric field was low until high biases resulting in

a sudden transition from initial states to confined states. In another experiment, it was shown that a small biased annulus could produce sheared flows within the main column of the plasma[14]. A new biasing mechanism has allowed for a continuous transition from a low flow shear state in the IDD—LAPD’s natural state—to a zero shear state, to a high shear state in the EDD. With this smooth control of flow shear, we can carefully observe the effect of shear on turbulent fluctuations, particle flux, and gradient length scale to a level of detail not yet previously achieved.

In this letter, we report on the observation of improved and degraded cross-field confinement as a function of sheared flow ranging from no shearing to up to five times a no-shear turbulent autocorrelation rate. This confinement occurs regardless of flow or flow shear direction and is demonstrated through both gradient scale length variation of density profiles and by turbulent particle flux measurements. We show that radial correlation length, particle flux, and density fluctuation power all decrease with shearing rate and decreases begin at rates less than the no-shear autocorrelation rate. The overall decrease in radial flux here is dominated by decreases in density fluctuations and radial correlation length of turbulent structures at frequencies less than 10kHz. In this range, crossphase between density and azimuthal electric field fluctuations remain near zero for all shearing rates which tends to maximize turbulent transport. We do note the emergence of a coherent mode at high shear with frequencies above 10kHz that originates in the region of peak flow. Fluctuations from this mode appear to increase density fluctuations above 10kHz, but do not

appear to contribute to flux as crossphase in this region is aligned to allow zero transport on average. We note that electric field fluctuations appear to be minimally affected by shearing changes. Lastly, we show fits of density fluctuations and radial correlation length to a power-law decay for comparison to theory [11].

The Large Plasma Device [15] (LAPD) is a 20m by 1m cylindrical linear device with a 54cm wide barium-oxide coated nickel cathode pulsed at 1Hz to produce a 45eV electron beam which ionizes the helium gas in the chamber. A column long plasma of density about $5 \times 10^{12} \text{ cm}^{-3}$ and temperature of 5eV is produced. The field for this experiment was set to 1000G. To produce the bias, four quarter annulus aluminum plates are inserted half a meter axially beyond the cathode creating an iris-like boundary condition between the cathode-anode and the main plasma chamber with a aperture of 26cm. A pulse power circuit connected to a capacitor bank supplies a 5ms bias during the 15ms plasma discharge. Bias ranges from a floating potential of 35V to 230V referenced from the cathode. Measurements of ion saturated current (i_{sat} —as a proxy for density) and floating potential are taken with a 9-tip flush surface tantalum probe while temperature and plasma potential is taken by swept Langmuir probe.

Azimuthal flow and flow shear are controlled by adjusting the voltage on the limiter plates. When voltages on the limiter on are less than the voltage of the anode—as is the case for LAPD’s spontaneous flow state—an overall azimuthal flow occurs in the IDD as shown in Fig. 1 with velocities peaking just outside the limiter edge. When the voltage on the limiter is brought near anode potential, flow and flow shear zero out. Voltages above anode produce electron diamagnetic direction flows peaked at the limiter edge. The voltage on the power supply cannot be set below the floating potential as the plasma tends to charge the capacitor banks.

Measurements of i_{sat} and particle flux are taken for each bias flow state. A set of radial values are averaged over a range from 27 to 31cm in a region where such averaged flow and flow shear scale approximately linearly with limiter bias Fig. 1 and are outside the limiter edge to avoid any possible effects from primary electrons. Maxing out at 125kHz, we produce a shearing rate of approximately five times the measured no-shear autocorrelation rate. An autocorrelation time of about $36\mu\text{s}$ is calculated by taking the full width at half max of a Hilbert transform of the i_{sat} autocorrelation function at the no flow/shear bias yielding a decorrelation rate of $\Delta\omega_t = 28\text{kHz}$.

Calculated quantites are used to characterize flux and length scale. Density gradient length scale is calculated by $L_n = |\nabla \ln n|^{-1}$ while particle flux, $\Gamma_p = \langle \tilde{n} \tilde{v}_r \rangle =$

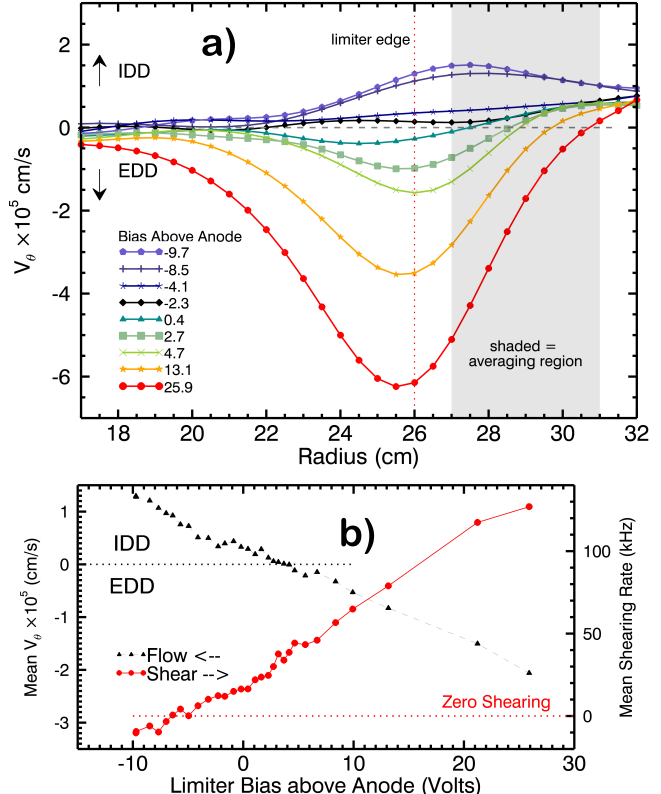


FIG. 1. (a) Velocity profiles using plasma potential from swept measurements. (b) Nearly linear scaling of flow (black) and shearing (red) versus limiter bias.

$\langle \tilde{n} \tilde{E}_\theta \rangle / B$, can be calculated spectrally as[16],

$$\Gamma_p = \frac{2}{B} \int_0^\infty |n(\omega)| |E_\theta(\omega)| \gamma_{n, E_\theta}(\omega) \cos[\phi_{n, E_\theta}(\omega)] d\omega \quad (1)$$

which also allows us to directly determine the contributions of turbulent fluctuations, crossphase and coherency to the particle flux.

The first clear result shown in Fig. 2 is a degradation of confinement from the spontaneous state followed by improved confinement as bias is increased, as indicated by a change in the gradient scale length of the density radial profiles. The average density gradient scale length begins at 9cm with no bias, but at the point of minimum shearing rate, the density gradient levels out, reaching a scale length peak of about 15cm. As bias increases, the density gradient steepens further saturating at about 5cm. The initial scale length value and saturated values are consistent with previous biasing experiments done on the LAPD[1], but rather than see a gradual change like here, a sharp threshold was observed. The new biasing setup allows this transition to be observed as its design allows for continuous variation of flow at the plasma edge. In the previous experiment that a threshold was observed not because of an inherent dependence on a shear value, but because of penetration of cross-field current—and thus flow—from the chamber edge to the plasma source. By placing the limiters closer to the core plasma edge edge,

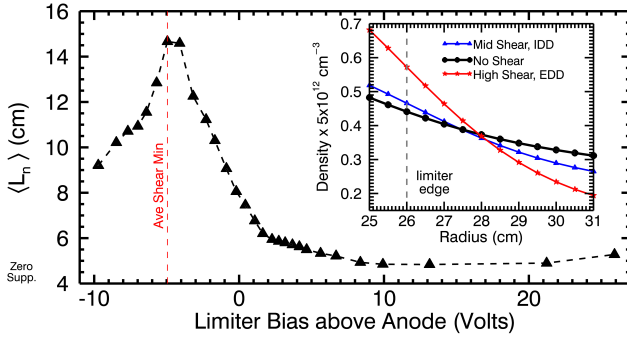


FIG. 2. Density gradient length scale versus limiter bias. Inset shows density profile relaxing then steepening again with bias.

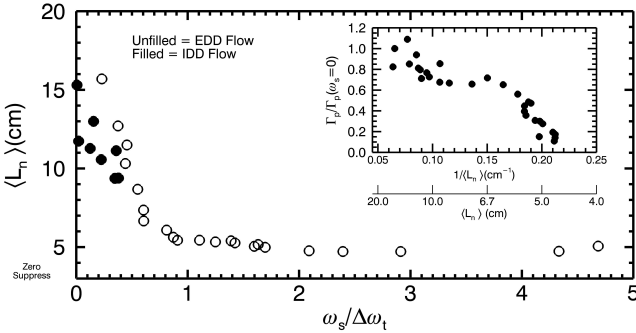


FIG. 3. Gradient scale length versus shearing rate. Inset shows correlation of gradient scale length and turbulent particle flux. Note how this data is inconsistent with a Fick's Law like diffusion, which would be identified by a linearly increasing flux with gradient.

we can establish cross-field currents at lower shear values than before.

Given the linear relationship between limiter bias and average shear flow, we can compare the variation in L_n to shearing rate, ω_s , normalized to $\Delta\omega_d$ as in Fig. 3. It is clear from this plot that confinement improvement begins immediately with shearing and reaches a saturated state for $\omega_s \approx \Delta\omega_d$ and that this transition occurs continuously and gradually. Also, improved confinement does not depend on flow direction as both IDD and EDD flow points lie on the same curve.

The change in confinement can be connected to a change in the turbulence properties of the plasma which dictate the turbulent flux. An overview of fluctuation power in isat can be seen in the spectrum of Fig. 4. Most of the fluctuation power is located less than 10kHz and that in this range, power decreases overall with increasing shearing rate. A decrease of about one order of magnitude is seen between the lowest shearing point and the high shear regime. Above 10kHz, power drops off considerably; however, beyond a normalized shearing value of 1.0, a coherent mode emerges with a frequency that begins at about 10kHz and increases linearly with shearing to a value of about 12kHz. The fluctuation power at these high shearing rates is almost entirely located within

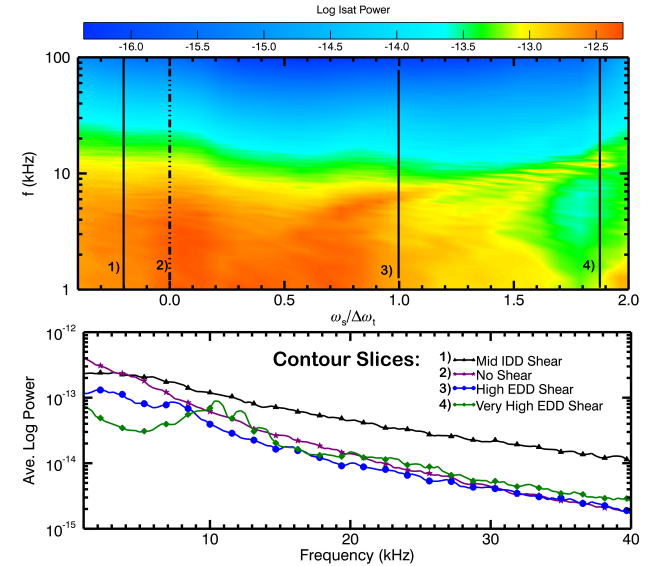


FIG. 4. Contour plot of log isat fluctuation power versus shearing rate and frequency. Dashed lines show location of decorrelation rate.

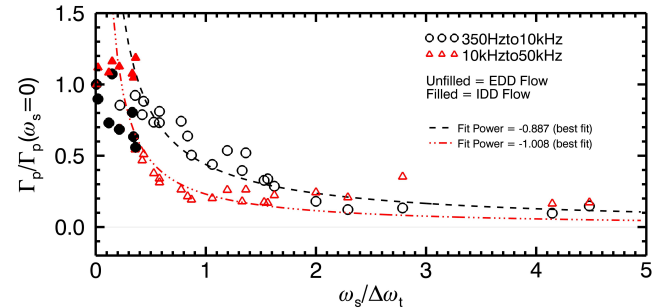


FIG. 5. Particle flux as a function of shearing rate normalized to decorrelation rate. Black points show low frequency, red shows high. Filled symbols represent points with flow in IDD.

this mode.

The changes in gradient scale length and turbulence are indicative of an overall change in particle flux. This flux can be directly measured by correlating fluctuating isat with fluctuating radial flow— $E \times B$ flow using an electric field derived from two floating potential tips on either side of the isat measuring tip and rewritten in terms of the integral in (1). Like gradient scale length, normalized average particle flux decreases with shearing rate as in Fig. 5; however, while flux decrease begin immediately with shearing, the decrease is not as fast as L_n with saturation not occurring until at least $\omega_s > 2\Delta\omega_d$. Flux decreases do not depend on flow direction either as again both IDD and EDD points fit on about the same curve.

Returning to fluctuations, the calculated flux can be analyzed by its fluctuation and phase components separately as in Fig. 6. The top two plots show fluctuation power—isat and azimuthal electric field (E_θ)—as functions of normalized shearing rate, while the bottom two

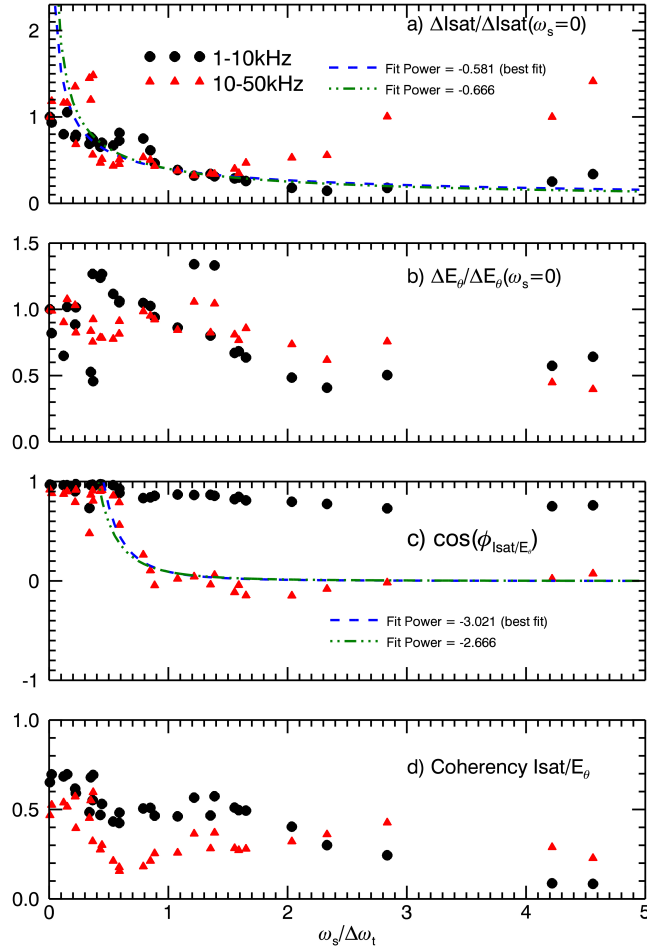


FIG. 6. Components of particle flux versus shearing rate including $\text{isat}/\text{Density}$ fluctuation power(a), electric field fluctuation power(b), crossphase(c) and coherency(d) with black points for low frequency, red for high.

show crossphase and coherency between the two fluctuating quantities. As expected from the power contour plot, isat fluctuations decrease with shearing with power concentrated in frequencies $\gtrsim 10\text{kHz}$. Concurrently, cosine of crossphase between isat and E_θ for this bandwidth remains steady at nearly 1. Thus, flux is predominately suppressed by decreases in isat fluctuations, not crossphase. Note, however, isat fluctuations appear to increase beyond a normalized shearing of 2.0. These increases, however, are almost entirely from $\gtrsim 10\text{kHz}$ contributions suggesting that they originate from the coherent mode. Comparing to Fig. 5, it is clear these fluctuations do not contribute to the flux. For high frequencies, $\cos(\phi_{\text{isat}, E_\theta})$ is zero for high shearing. Thus, despite increase fluctuations, no overall flux is observed.

As predicted by early theories on shear suppression, the effect of decreasing fluctuations is related to the shortening of a radial correlation length for turbulent structures. Using a cross-correlation technique, we observe this precise modification of turbulent structures by azimuthal shearing as shown in Fig. 7. The radially corre-

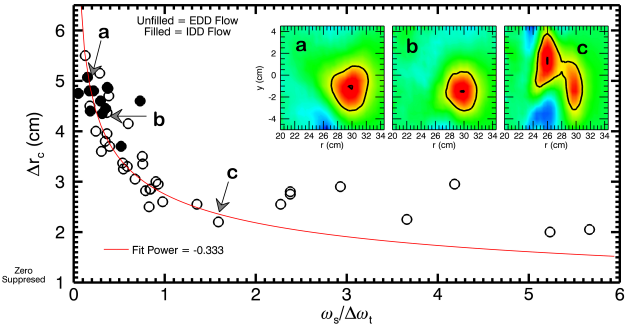


FIG. 7. Measured radially correlation length with reference probes at 28, 29, 30, 31 or 32 cm and shows a decrease with flux that can be nearly fit to a power-law of $-1/3$. Inset shows 2D correlation length with reference probe at 30 cm in azimuthal plane for low IDD flow shearing, no shear and high EDD flow shearing. The decrease in radial correlation can be seen as well as slight tilting depending on the direction of shear. A mode appears at higher shearings which appears to slightly extend correlation length.

lation length here is defined as the width of the contour plot to decrease to one-half its maximum value which occurs at the reference point, represented by the black curve in the inset of Fig. 7. Like the flux and fluctuation data, the suppression begins with relatively little shearing and approaches a saturated value, though unlike flux, there appears to be a slight asymmetry in widths for IDD and EDD. This may be due to the influence of a coherent mode. In the high shearing regime, a mode pattern is clearly observed located in the peak EDD flow region and is distinct from the correlation structure. A similar mode may be present in the IDD flow region, but is more difficult to distinguish from the correlation structure adding to the apparent correlation width.

Lastly, we can compare some of our results to theory. The BDT model uses a basis of shear effecting eddy step size to produce a power-law scaling of the form $(\omega_s/\Delta\omega_t)^{-\alpha}$ for density fluctuations and radial correlation length versus normalized shearing. A comparison of the power fit to the predicted exponent is made for each quantity. As seen in Fig. 6 a best fit of $\alpha = 0.530$ compares favorably to the BDT prediction of $\alpha = 2/3$. Similarly, a fit of $\alpha = 999999$ for radial correlation lenght in Fig. 7 compares well to the BDT prediction of $\alpha = 1/3$. A cavaet though is BDT theory is based on a constant density gradient while here gradients are always changing. Nevertheless, this initial agreement of data to model is promising for future comparisons.

This letter presents the first continuous variation shearing rate in a plasma device and has shown a clear effect of particle flux and density confinement through both the mechanisms of turbulent fluctuation and radial correlation length reduction.

-
- [1] T. Carter and J. Maggs, Phys. Plasmas **16**, 012304 (2009).
- [2] F. Wagner and et al., Phys. Rev. Lett. **49**, 1408 (1982).
- [3] R. Taylor, M. Brown, B. Fried, H. Grote, J. Liberati, G. Morales, P. Pribyl, D. Darrow, and M. Ono, Phys. Rev. Lett. **63**, 2365 (1989).
- [4] G. Tynan, L. Schmitz, R. Conn, R. Doerner, and R. Lehmer, Phys. Rev. Lett. **68**, 3032 (1992).
- [5] R. Groebner, K. Burrell, and R. Seraydarian, Phys. Rev. Lett. **64**, 3015 (1990).
- [6] R. Moyer and et al., Phys. Plasmas **2**, 2397 (1995).
- [7] G. Tynan, C. Holland, J. H. Yu, A. James, D. Nishijima, M. Shimada, and N. Taheri, Plasma Phys. Control Fusion **48**, S51 (2006).
- [8] J. Boedo, D. Gray, S. Jachmich, R. Conn, G. Terry, G. Tynan, G. V. Oost, R. Weynants, and T. Team, Nucl. Fusion **40**, 7 (2000).
- [9] J. Maggs, T. Carter, and R. Taylor, Phys. Plasmas **14**, 052507 (2007).
- [10] R. Weynants and G. V. Oost, Plasma Phys. Control Fusion **35**, B177 (1993).
- [11] H. Biglari, P. Diamond, and P. W. Terry, Phys. Fluids B, **2**, 1 (1990).
- [12] A. Ware, P. Terry, P. Diamond, and B. Carreras, Plasma Phys. Control Fusion **38**, 1343 (1996).
- [13] P. Terry, D. Newman, and A. Ware, Phys. Rev. Lett. **87**, 18 (2001).
- [14] S. Zhou, W. Heidbrink, H. Boehmer, R. McWilliams, T. Carter, S. Vincena, B. Friedman, and D. Schaffner, Phys. Plasmas **19**, 012116 (2012).
- [15] W. Gekelman, H. Pfister, Z. Lucky, J. Bamber, D. Lenneman, and J. Maggs, Rev. Sci. Instrum. **62**, 2875 (1991).
- [16] E. Powers, Nucl. Fusion **14**, 749 (1974).